

# Application of IR imaging for free-surface velocity measurement in liquid-metal systems

M. G. Hvasta,<sup>a)</sup> E. Kolemen, and A. Fisher  
 Princeton University, Princeton, New Jersey 08544, USA

(Received 27 September 2016; accepted 16 December 2016; published online 5 January 2017)

Measuring free-surface, liquid-metal flow velocity is challenging to do in a reliable and accurate manner. This paper presents a non-invasive, easily calibrated method of measuring the surface velocities of open-channel liquid-metal flows using an IR camera. Unlike other spatially limited methods, this IR camera particle tracking technique provides full field-of-view data that can be used to better understand open-channel flows and determine surface boundary conditions. This method could be implemented and automated for a wide range of liquid-metal experiments, even if they operate at high-temperatures or within strong magnetic fields. *Published by AIP Publishing.* [<http://dx.doi.org/10.1063/1.4973421>]

## I. INTRODUCTION

Flowing liquid-lithium plasma facing components (FLL-PFC's) provide an attractive alternative to solid PFC's traditionally used in fusion reactors. FLL-PFC's possess excellent heat-transfer and power-removal characteristics, permit PFC exposure to large heat-fluxes, provide a self-healing surface that is immune to both thermal stresses and radiation damage, and facilitate tritium breeding.<sup>1</sup> Additionally, several experiments have shown that FLL-PFC's improve plasma performance within tokamaks by increasing energy confinement, reducing particle recycling, and suppressing impurity emissions.<sup>2-4</sup>

A major challenge facing FLL-PFC development is the accurate and reliable measurement of free-surface, liquid-metal velocities. There are several well-known techniques for measuring liquid-metal velocities within pipes and tubes,<sup>5</sup> but none of these methods can be easily modified to measure flow velocities on FLL-PFC surfaces exposed to fusion reactor operating conditions (high-temperatures, strong magnetic fields, radiation exposure, high-vacuum, etc.). Therefore, this paper will focus on the development of a non-contact, non-invasive particle tracking technique that uses an infrared (IR) camera to take velocity measurements relevant to FLL-PFC's.

## II. EXPERIMENT OVERVIEW

The Liquid Metal eXperiment (LMX)<sup>6,7</sup> was created to study free-surface, liquid-metal flows and magnetohydrodynamic effects relevant to FLL-PFC development. During LMX operation, an alloy commonly known as "galinstan" ( $\text{Ga}^{67}\text{In}^{20.5}\text{Sn}^{12.5}$  wt. %) was pumped into the bottom of a rectangular open-channel and then circulated through the rest of the system, as depicted in Fig. 1. The outside of the channel was made from 316SS. The interior of the channel was lined with acrylic in order to electrically isolate the galinstan from

the channel. For this paper, a weir (approximately 0.6 cm tall) was used to maintain a minimum depth in the open-channel before allowing the galinstan to overflow, drain into the pumped portion of the system, and then return to the channel.

## III. PUMP AND FLOWMETER

Galinstan was pumped through LMX using a custom-made, Archimedes-style screw pump. The pump was powered by a 2 HP Leeson DC motor while the rotations per minute (RPM) were monitored using an Extech 461950 tachometer. Liquid-metal flow through the tubes feeding the open-channel was measured using an FMG83 electromagnetic flowmeter from Omega Engineering. As shown in Fig. 2, the pump was able to reliably generate flow rates ranging from 4 to 10 l/min.

## IV. DEPTH MEASUREMENT

The depth of the flowing galinstan was measured in the center of the channel (5.45 cm away from either wall) using the electrical contact probe method,<sup>8</sup> which is depicted in Fig. 3. When depth measurements were taken, one probe was kept in contact with the galinstan while the other was moved vertically in the gas-space above the liquid-metal. When the rounded-bottom of the moveable probe touched the surface of the galinstan, the multimeter indicated a change from an "open" to a "closed" circuit. An operator manually adjusted the height of the probe during an experiment to change the output of the multimeter and determine the location of the liquid-metal surface.

An Aerotech ATS-300 translation stage was used to move the electric contact probe above the surface of the liquid metal. A vernier scale was used to measure where the probe came into contact with the surface of the galinstan with 0.1 mm resolution. As shown in Fig. 4, above 1000 RPM the galinstan flowed smoothly over the weir and the depth could be accurately modeled using a polynomial fit. Visual inspection during operation indicated that the fluid depth across the duct

<sup>a)</sup>Author to whom correspondence should be addressed. Electronic mail: MHvasta@princeton.edu

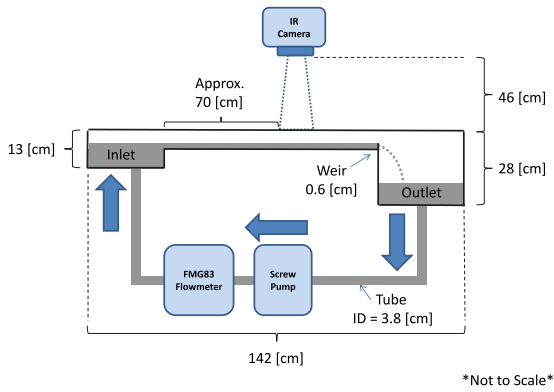


FIG. 1. A simple depiction of the LMX flow path and instrumentation layout. The width of the channel ( $w$ ) was a constant 10.9 cm.

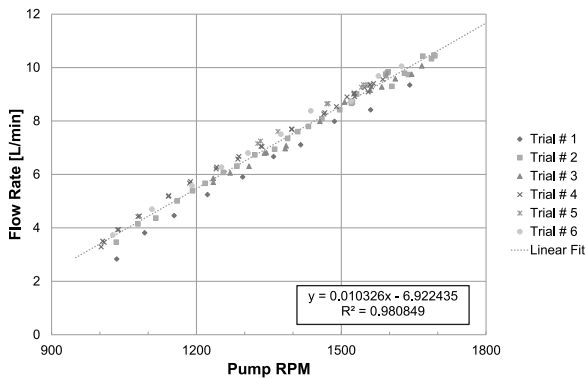


FIG. 2. Pump output as measured by the electromagnetic flowmeter. The flowmeter data closely agree with a linear fit. Pump data were collected over several weeks of operation.

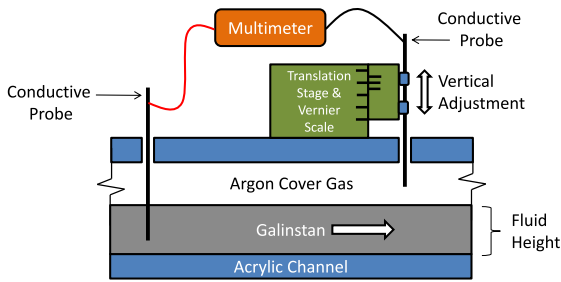


FIG. 3. A depiction of the electrical contact probe setup used to measure the location of the liquid-metal surface.

was largely uniform and no appreciable wall- or edge-effects were seen.

During these tests, the width of the channel ( $w$ ) was held at a constant 10.9 cm. Since both liquid depth ( $h$ ) and flow rate ( $Q$ ) were known as a function of pump RPM, the average velocity ( $v_{avg}$ ) of the galinstan could be calculated using the following equation:

$$Q = v_{avg} hw. \quad (1)$$

### V. INFRARED PARTICLE TRACKING

During LMX operation, oxidation of the galinstan was minimized by keeping the gas-space above the open-channel inerted with ultra-high purity argon. However, despite efforts

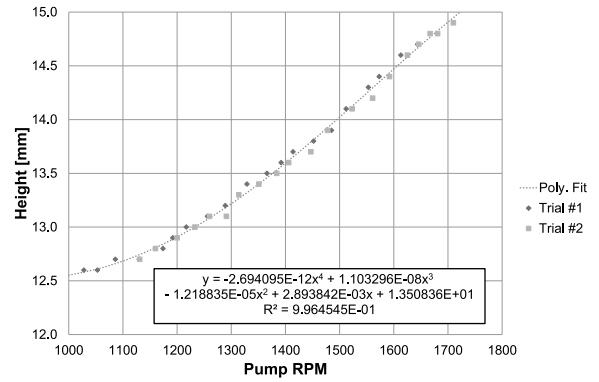


FIG. 4. The height of the flowing galinstan surface as a function of pump RPM. Data were collected using the electrical contact method. Above 1000 RPM, the galinstan began to flow over the weir and circulate through the system. The surface of the galinstan rises above the weir before beginning to flow due to surface tension effects ( $\gamma = 0.533$  N/m).<sup>6,7</sup>

to maintain cleanliness, small amounts of impurities would develop and float along the surface of the galinstan.<sup>6</sup> These impurities were used as tracers during this experiment and no additional particles were intentionally added.

While the galinstan was flowing, it was challenging to see the small ( $<1$  mm), intermittently occurring oxide particles with the naked-eye or capture them with a CCD camera unless they were illuminated with a light source<sup>9</sup> or laser-sheet,<sup>10</sup> which can be spatially limited or difficult to aim exactly where needed. However, due to the thermal and optical differences between the matte oxides and the mirror-like galinstan,<sup>11–14</sup> an IR camera could be used to resolve and track the impurities being carried by the flowing galinstan, as shown in Fig. 5. This method does not require any temperature gradients in the liquid metal or temperature differences between the liquid metal and impurities.<sup>15</sup>

A FLIR SC5000 ( $640 \times 512$  pixels, 60 Hz) IR camera was used to film the surface of the flowing galinstan over the full range of flow rates. The average velocities of the impurity tracer particles were manually calculated using the pixel data embedded in the videos with the following equation:

$$v_{surf} = K(x_1 - x_0)/(t_1 - t_0), \quad (2)$$

where  $K$  is a coefficient to scale from pixels to actual distance,  $x$  is the pixel location of the tracer particle, and  $t$  is the timestamp on the IR camera footage. For this experiment, the

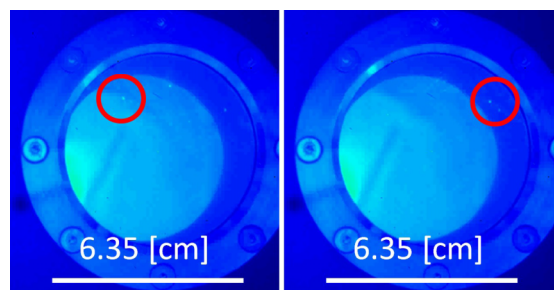


FIG. 5. A sample of data collected using the IR camera particle tracking method. IR compatible windows were installed above the free-surface flow. Left timestamp = 2.04 s, right timestamp = 4.20 s.

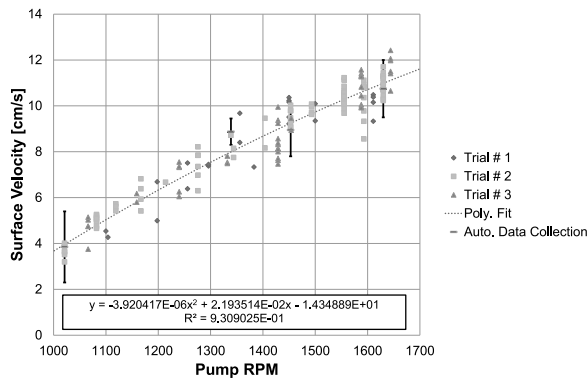


FIG. 6. The surface velocity of the galinstan flow as measured using the IR camera particle tracking technique. Tracer particle velocities were measured near the center of the channel. The polynomial fit was produced using the manually collected data. Error bars on the “Auto. Data Collection” data set show the standard deviation of the velocities measured by the software. Automatic data collection was not performed for all data sets.

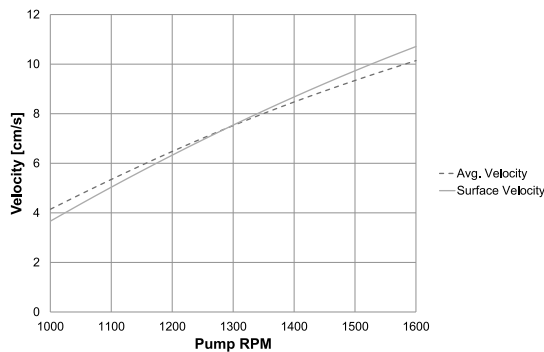


FIG. 7. A comparison of the average and surface velocities. The values shown above were calculated using the linear and polynomial fits given in Figs. 2, 4, and 6.

spatial resolution of the camera was  $K = 0.027$  cm/pixel and timestamp data were rounded to the nearest 1 ms. As shown in Fig. 6, the IR camera particle tracking data yielded consistent results between test runs. Data collected manually using the FLIR software package agreed closely with results generated by PTVlab,<sup>16</sup> a specialized particle-tracking software package that enabled automated data collection.

## VI. VELOCITY MEASUREMENT COMPARISON

To validate the data collected using the particle tracking technique, the surface velocity measurements were compared to the bulk velocity measurements. As shown in Fig. 7, the average velocity of the galinstan in the open-channel agreed closely with the surface velocity of the liquid metal. The maximum difference between the two fits was 11.6%, which occurred at 1000 RPM.

## VII. SUMMARY AND DISCUSSION

A non-invasive, easily calibrated method of measuring the surface velocity of liquid-metal flows using a commercially available IR camera was presented. Unlike spatially limited laser-sheet methods, the IR camera particle tracking

technique provides full field-of-view data that could be used to better understand open-channel flows. Additionally, unlike ultrasonic velocimetry techniques,<sup>17</sup> this new technique is unaffected by oxide build-up or acoustic interface issues between the vessel wall, the liquid metal, and the air or argon in the gas-space.

This method could be implemented and automated within fusion reactors equipped with FLL-PFC’s. Due to the reactive or “gettering” nature of alkali metals<sup>2,3,18</sup> and the optical differences between lithium, the corresponding oxides, hydroxides, and nitrides,<sup>19,20</sup> it is possible that tracer particles will not need to be intentionally added during reactor operation.

The flow velocities measured by the particle tracking technique closely matched those measured using a commercially available electromagnetic flowmeter. However, the two methods did not generate data that could be easily correlated using a constant offset or correction coefficient. As shown in Fig. 7, for pump speeds above 1300 RPM the surface velocity became greater than the average velocity, as would be expected for most open channel flows.<sup>21,22</sup> Meanwhile, at lower pump speeds, the surface velocity lagged the average velocity. This phenomenon could be due to surface tension effects becoming overpowered by inertial effects at higher flow rates. Evidence supporting this possibility was seen during numerous tests where the surface oxides on the galinstan did not move at all for small flow rates. Alternatively, this trend could be due to other hydrodynamics that are beyond the scope of this paper. Suffice it to say, for this experiment, the particle tracking technique yielded similar results to the bulk velocity measurements but future analysts must realize that surface velocity measurements may not easily or neatly correspond to bulk fluid velocities.

Future plans for LMX will implement this technique to better understand the effects of magnetic fields and Lorentz forces on open-channel galinstan flows.

## ACKNOWLEDGMENTS

The research described in this paper was conducted under the Laboratory Directed Research and Development Program (LDRD) at Princeton Plasma Physics Laboratory, a national laboratory operated by Princeton University for the U.S. Department of Energy under Prime Contract No. DE-AC02-09CH11466.

The authors would also like to thank E. Gilson, H. Ji, K. Caspary, P. Sloboda, and M. Jaworski for their expertise, assistance, and insights during these experiments.

The digital data for this paper can be found at: <http://arks.princeton.edu/ark:/88435/dsp01x920g025r>.

<sup>1</sup>R. E. Nygren, T. D. Rognlien, M. E. Rensink, S. S. Smolentsev, M. Z. Youssef, M. E. Sawan, B. J. Merrill, C. Eberle, P. J. Fogarty, B. E. Nelson, D. K. Sze, and R. Majeski, *Fusion Eng. Des.* **72**, 181 (2004).

<sup>2</sup>R. Maingi, D. P. Boyle, J. M. Canik, S. M. Kaye, C. H. Skinner, J. P. Allain, M. G. Bell, R. E. Bell, S. P. Gerhardt, T. K. Gray, M. A. Jaworski, R. Kaita, H. W. Kugel, B. P. LeBlanc, J. Manickam, D. K. Mansfield, J. E. Menard, T. H. Osborne, R. Raman, A. L. Roquemore, S. A. Sabbagh, P. B. Snyder, and V. A. Soukhanovskii, *Nucl. Fusion* **52**, 083001 (2012).

<sup>3</sup>J. S. Hu, G. Z. Zuo, J. Ren, Q. X. Yang, Z. X. Chen, H. Xu, L. E. Zakharov, R. Maingi, C. Gentile, X. C. Meng, Z. Sun, W. Xu, Y. Chen, D. Fan, N. Yan,

- Y. M. Duan, Z. D. Yang, H. L. Zhao, Y. T. Song, X. D. Zhang, B. N. Wan, J. G. Li, and E. A. S. T. Team, *Nucl. Fusion* **56**, 046011 (2016).
- <sup>4</sup>J. Ren, J. S. Hu, G. Z. Zuo, Z. Sun, J. G. Li, D. N. Ruzic, and L. E. Zakharov, *Phys. Scr.* **T159**, 014033 (2014).
- <sup>5</sup>G. E. Turner, *Liquid Metal Flow Measurement (Sodium) State-of-the-Art-Study, LMEC-Memo-68-9* (Liquid Metal Engineering Center, 1968).
- <sup>6</sup>M. D. Nornberg, H. Ji, J. L. Peterson, and J. R. Rhoads, *Rev. Sci. Instrum.* **79**, 094501 (2008).
- <sup>7</sup>J. R. Rhoads, Ph. D. dissertation (Princeton University, 2013), <http://arks.princeton.edu/ark:/88435/dsp01rj430467r>.
- <sup>8</sup>H. W. Slocumb, *Liquid Metal Level Measurement (Sodium) State-of-the-Art-Study, NAA-SR-MEMO-12582* (Liquid Metal Engineering Center, 1967).
- <sup>9</sup>M. A. Jaworski, T. K. Gray, M. Antonelli, J. J. Kim, C. Y. Lau, M. B. Lee, M. J. Neumann, W. Xu, and D. N. Ruzic, *Phys. Rev. Lett.* **104**, 094503 (2010).
- <sup>10</sup>M. Narula, A. Ying, and M. A. Abdou, *Fusion Sci. Technol.* **47**, 564–568 (2005).
- <sup>11</sup>Pure galinstan has a very high reflectivity<sup>12,13</sup> and a very low emissivity<sup>14</sup> ( $\epsilon \approx 0.04$ ). By comparison, the measured emissivity of the impurities ranged from 0.73 to 0.99.
- <sup>12</sup>L. A. Akashev and V. I. Kononeko, *Tech. Phys.* **43**, 118 (1998).
- <sup>13</sup>E. F. Borra, G. T. Tremblay, Y. Huot, and J. Gauvin, *Astron. Soc. Pac.* **109**, 319–325 (1997).
- <sup>14</sup>A. Arthurs, J. Rhoads, E. Edlund, E. Spence, and H. Ji, in *Measurement of the Emissivity of Liquid Gallium Alloy for Temperature Measurements of Free-Surface Flows*. 52nd Annual Meeting of the APS Division of Plasma Physics, Chicago, IL, 2010.
- <sup>15</sup>D. N. Ruzic, W. Xu, D. Andruczyk, and M. A. Jaworski, *Nucl. Fusion* **51**, 102002 (2011).
- <sup>16</sup>A. Patalano and B. Wernher, PTVlab—Time-Resolved Digital Particle Tracking Velocimetry (PTV) Tool for Matlab, V.1.2, 2009.
- <sup>17</sup>D. Brito, H. Nataf, P. Cardin, J. Aubert, and J. Masson, *Exp. Fluids* **31**, 653–663 (2001).
- <sup>18</sup>R. Bastasz and J. A. Whaley, *Fusion Eng. Des.* **72**, 111–119 (2004).
- <sup>19</sup>M. A. Jaworski, T. Abrams, J. P. Allain, M. G. Bell, A. Diallo, T. K. Gray, S. P. Gerhardt, R. Kaita, and H. W. Kugel, *Nucl. Fusion* **53**, 083032 (2013).
- <sup>20</sup>P. Fiffis, T. W. Morgan, S. Brons, G. G. Van Eden, M. A. Van Den Berg, W. Xu, D. Curreli, and D. N. Ruzic, *Nucl. Fusion* **55**, 113004 (2015).
- <sup>21</sup>N. Cheng, *Adv. Water Resour.* **30**, 1775–1784 (2007).
- <sup>22</sup>C. Chiu, *J. Hydraul. Eng.* **5**, 576–594 (1989).